Quantized motion of atoms in a quadrupole magnetostatic trap

T. H. Bergeman, Patrick McNicholl,* Jan Kycia,† Harold Metcalf, and N. L. Balazs

Department of Physics, State University of New York, Stony Brook, New York 11794

Received April 5, 1989; accepted July 10, 1989

We consider quantized motion of neutral atoms cooled below the recoil limit in a quadrupole magnetostatic trap. Because of Majorana transitions to untrapped levels near the point of zero field at the trap center, all quantum levels have a nonzero decay rate. The Schrödinger equation associated with the potential $g\mu\mathbf{B}\cdot\mathbf{S}$ ($\mathbf{S}$ is the total atomic spin) takes the form of coupled equations in r when the spinor components are expanded in spherical harmonics. We integrate the multichannel problem numerically to obtain asymptotic phase shifts, resonance energies, and widths. For $S = 1/2$, the lowest levels have widths somewhat less than their spacing. Thus the trap quantum-level structure might possibly be observable if the atoms are sufficiently cold, namely, in the 0.1-μK regime for most atoms and attainable trap field gradients. The width decreases rapidly with increasing M_J, the angular momentum about the symmetry axis. Spectroscopic linewidths of a few hertz are possible if there is enough population in the lowest levels with a few M_J quanta. The decay rate of the lowest levels, however, is probably too rapid for studying Bose–Einstein condensation in such a trap.

1. INTRODUCTION

This is a study of quantized atomic motion in the quadrupole (two-coil) magnetostatic trap. At present, the energy regime for which quantization is significant is below the lowest temperatures attained. However, in view of recent surprising progress in cooling neutral atoms,[1–3] it seems reasonable to think about what may lie ahead. The quantum-level structure is of interest in the proposed investigation of Bose–Einstein condensation of trapped atoms[4] into the lowest quantum level and also with regard to possibilities for overcoming Zeeman broadening of spectroscopy transitions of the magnetically trapped atoms.

The peculiar aspect of atomic motion in a magnetostatic trap that makes the problem nontrivial is the possibility of Majorana transitions from one Zeeman sublevel to another, occurring as the atom moves through a field that varies in magnitude and direction over space. As long as the field magnitude is sufficiently large that the Larmor precession period is short compared with the time in which the atom sees a significant change of field direction, the atom remains in the Zeeman sublevel that is trapped. Hence Majorana transitions can essentially be avoided in traps with a nonzero minimum, such as Ioffe-type configurations[5,6] (in which straight conductors produce fields that confine axially and coils are used for longitudinal confinement) and the baseball coil trap.[6]

The quadrupole trap[7] possesses certain advantages that make it worthy of study even though the Majorana transition problem is raised most severely. The construction of quadrupole (two-coil) traps is relatively simple, and the quantum levels are spaced farther apart than in the $|\mathbf{B}|_{\min} \neq 0$ traps because the potential varies linearly near the center rather than quadratically. For quadrupole traps, however, the zero of field at the center necessarily leads to a violation of the adiabaticity condition. The possibility of detecting Bose–Einstein condensation in such a trap therefore depends on whether the decay rate out of the lowest level is rapid compared with the time of observation. Also, the intrinsic linewidth of the trap quantum states will affect the theoretical minimum width of spectroscopic and clock transitions of atoms in the trap.

Aside from practical implications, the new questions of physics that arise provide another motivation for studying the quantization of motion in the trap. Because the forces in a magnetostatic trap depend on the atom's internal spin, *the traditional factorization of space and spin variables does not apply*, so there are certain challenges to mathematical physics. A stimulus to facing these questions arises from the recently developed experimental techniques actually to observe transitions between Zeeman sublevels of trapped atoms, using optical detection.[8] These techniques may be suitable for detecting the quantized levels, provided that the temperature of the trapped atoms is low enough.

The present study is preliminary in several respects. Atoms with an internal spin of 1/2 are the primary subject of study, although as of now no such atoms have been trapped. Even hydrogen has total spin (nuclear spin plus electron spin) of 0 or 1, while rubidium and sodium have total spins of 1 to 4 in the ground electronic state. The problem presented by atoms with spins larger than 1/2 requires more channels and more time-consuming calculations. It was believed most important to deal first with the basic issues simply in the context of the $S = 1/2$ atoms. However, results for spin 1 and spin 2 in an approximation that neglects transitions to untrapped, continuum states are presented. Other questions that we do not discuss are the spectral intensities that one might observe in microwave transitions from one hyperfine level to another and the means of cooling atoms within the trap to a temperature such that the spectral lines are not impossibly dense.

Although there are relatively few cases in which space and spin do not factorize, there is an approximate analogy with molecular potential curves, in which the energy depends on

0740-3224/89/112249-08$02.00

the orientation of the spin and angular momentum with respect to the molecular axis. The coupled linearly rising and falling effective potentials in the trap are somewhat analogous to crossings of molecular potential curves, which can lead to quasi-stable states above the crossing.[9] In fact, the numerical methods employed here originate in research on diatomic potential problems. (Atom traps have been referred to as "one atom molecules."[10]) Other related problems are posed by the motion of atoms with spin through spatially varying fields in connection with Majorana transitions,[11] detailed models of the Stern–Gerlach effect,[12,13] and certain phenomena in neutron interferometry.[14,15] These discussions touch on certain facets of the problem of interest here.

2. THE HAMILTONIAN

The interaction energy for a trapped atom is given by

$$V = -\mathbf{B}\cdot\mu, \tag{1}$$

where μ is the magnetic moment of the atom. For purposes of this discussion, the total (internal) angular momentum of the atom is denoted here by the operator $\mathbf{S}$, which is normally used to denote the electron spin only. $\mathbf{S}$, which is normally denoted $\mathbf{F}$, is composed of electron spin $\mathbf{S}_e$, nuclear spin $\mathbf{I}_N$, and possibly electron angular momentum $\mathbf{L}_e$:

$$\mathbf{S} = \mathbf{F} = \mathbf{S}_e + \mathbf{I}_N + \mathbf{L}_e. \tag{2}$$

Hence, in terms of the Bohr magneton μ_B, and the atomic g factor $g_S = g_F$,

$$\mu = g_S\mu_B\mathbf{S}. \tag{3}$$

The orbital angular momentum of the atom about the trap center is denoted $\mathbf{L}$ (no subscript), while $\mathbf{J} = \mathbf{L} + \mathbf{S}$ represents the total angular momentum of the atom about the trap center.

For the quadrupole trap, shown schematically in Fig. 1, the components of magnetic field near the origin may be written[6] in terms of the field gradient near the origin, denoted a:

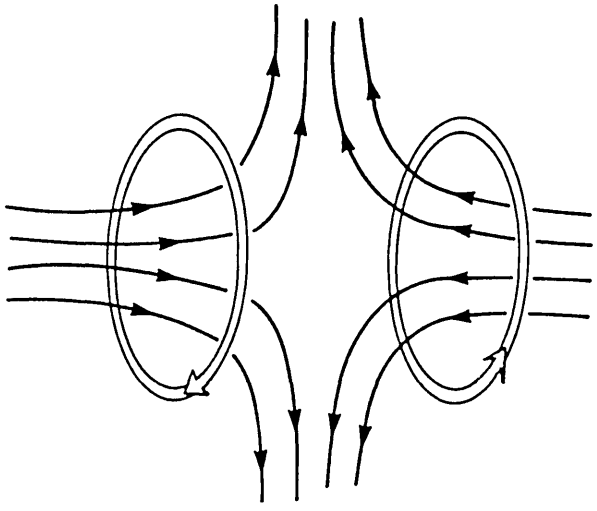

Fig. 1. Schematic diagram of the coil configuration used in the quadrupole trap and the resultant magnetic field vectors. Because the currents in the two coils are in opposite directions, there is a $\mathbf{B} = 0$ point at the center.

$$B_x = -\frac{ax}{2} = -\frac{ar\sin\theta\cos\phi}{2},$$

$$B_y = -\frac{ay}{2} = -\frac{ar\sin\theta\sin\phi}{2},$$

$$B_z = az = ar\cos\theta. \tag{4}$$

For an atom of mass M, the Schrödinger equation for a trapped atom is

$$\left(\frac{\hbar^2}{2M}\nabla^2 + E + g_S\mu_B\mathbf{B}\cdot\mathbf{S}\right)\psi = 0. \tag{5}$$

This reduces to a dimensionless form on the introduction of scaled variables $r \to x_0 r$, $E \to \epsilon_0 E$, and a reduced field vector, $\mathbf{b} = \mathbf{B}/ar$:

$$[\nabla^2 + 2(E + r\mathbf{b}\cdot\mathbf{S})]\psi = 0. \tag{6}$$

In constructing solutions to Eq. (6), it is useful to note that the conserved quantity is $M_J = M_S + M_L$, the sum of the internal and center-of-mass angular momentum along the coil axis.

The trap units that one obtains are

$$\text{unit of distance} = x_0 = \left(\frac{\hbar^2}{M\mu a}\right)^{1/3},$$

$$\text{unit of energy} = \epsilon_0 = \left[\frac{(\mu a\hbar)^2}{M}\right]^{1/3}. \tag{7}$$

These quantities indicate the general scale of the quantum states and hence are of interest even apart from the detailed solution. Attainable values for the field gradient a are 100 G/cm for conventional magnets and possibly 1000 G/cm for superconducting magnets. x_0 and ϵ_0 depend on g_S through μ and hence on the symmetry of the atomic state. Values for x_0 and ϵ_0 for $a = 100$ G/cm are listed in Table 1 for the ground states of hydrogen and the alkali atoms and for the $2\,^3S$ state of helium, which has also been proposed for trapping.[16] A trap energy unit of 2 kHz corresponds to $\sim$0.1 μK, so the temperature scale is extremely low in all cases. As the above expressions indicate, a lighter atom will have more widely separated quantum levels but only proportional to $M^{-1/3}$. On the other hand, the recoil energy [$E_{\text{recoil}} = h/(2M\lambda^2)$ Hz, in frequency units, for a resonance transition of wavelength λ] for laser cooling is inversely proportional to atomic mass. Hence the better ratios of trap unit to recoil energy happen to be for the heavier atoms, as shown in Table 1. A steeper field gradient increases the unit of energy by $a^{2/3}$. The structure of the trap quantum levels depends also on the multiplicity of the trapped state, $2S + 1$, as discussed below.

By applying an appropriate sequence of rotation operators, it is possible to diagonalize the potential matrix in Eq. (6). This approach is discussed in Section 4 and will be useful for computing discrete eigenfunctions and eigenvalues neglecting transitions to untrapped sublevels.

Diagonalizing V, however, does not simplify the solution of Eq. (6) when continuum levels are included. As discussed below and in Appendix A, such a transformation introduces a singularity at the origin for $M_J = S$ states. These states have nonzero probability at the origin where the probability of Majorana transitions is unity. And for states with $M_J > S$, an additional diagonalization of V is necessary to define the asymptotic form of the wave function components. In

Table 1. Trap Units of Distance and Energy for Several Atomic States of Interest Based on Eqs. (7) with the Field Gradient $a = 100$ G/cm[a]

Atom	State	$\lvert g_F\rvert$	x_0 (μm)	ϵ_0 (kHz)	λ (nm)	E_{recoil} (kHz)
^{1}H	$1\,^2S(F=1)$	1	0.90	12.5	122	13 300
^{4}He	$2\,^3S(J=F=1)$	2	0.45	12.5	1083	42.5
^{6}Li	$2\,^2S(F=1/2, 3/2)$	2/3	0.57	5.27	671	73.7
^{7}Li	$2\,^2S(F=1, 2)$	1/2	0.59	4.13	671	63.2
^{23}Na	$3\,^2S(F=1, 2)$	1/2	0.40	2.78	589	25.0
^{39}K	$4\,^2S(F=1, 2)$	1/2	0.33	2.33	766	8.72
^{85}Rb	$5\,^2S(F=2, 3)$	1/3	0.29	1.37	780	3.86
^{87}Rb	$5\,^2S(F=1, 2)$	1/2	0.26	1.79	780	3.77
^{133}Cs	$6\,^2S(F=3, 4)$	1/4	0.28	0.98	852	2.07

[a] For the two hyperfine doublets ($F = I \pm 1/2$) in the alkali ground states, g_F differs only in sign. (g_F is negative for $F = I - 1/2$.) For comparison, the last column gives the recoil energy for the resonance line with wavelength indicated in the preceding column.

the approach described in Section 3, the L, M matrix representation of V is obtained before diagonalization.

One question that arises in considering the motion of atoms in a magnetic field is the possibility of multivaluedness in the phase of the wave function owing to phase accumulation in successive orbits, as discussed by Berry[17] in other contexts. For purposes of the present discussion, however, it can be shown that this interesting phenomenon is not relevant.

3. CALCULATION OF THE ASYMPTOTIC PHASE-SHIFT MATRIX

In this section we develop a general formalism and occasionally specialize to the case $S = 1/2$ for clarity. Since Eq. (6) includes spin operators, the wave function ψ will contain spinors, denoted η. Our notation will follow standard usage:

$$\eta(\alpha)_\beta = \delta(\alpha, \beta). \tag{8}$$

For $S = 1/2$,

$$\eta(+) = \begin{bmatrix}1\\0\end{bmatrix}, \qquad \eta(-) = \begin{bmatrix}0\\1\end{bmatrix}. \tag{9}$$

Contraction over spinor indices gives

$$\sum_\beta \eta(\alpha')_\beta{}^\dagger \eta(\alpha)_\beta = \delta(\alpha', \alpha). \tag{10}$$

The product $\eta^\dagger A$ of a spinor with a matrix over spin space will be understood as

$$\sum_{\beta'} \eta(\alpha)_{\beta'}{}^\dagger A_{\beta'\beta} = A_{\alpha\beta}. \tag{11}$$

We can now write ψ as a spinor times an expansion whose terms contain radial wave functions and spherical harmonics:

$$\psi_\alpha = \eta(\alpha) r^{-1} \sum_L^{L_{\max}} R(r)_{L\alpha} Y[L, M_L(\alpha); \theta, \phi] \times \delta[M_J - M_S(\alpha) - M_L(\alpha)]. \tag{12}$$

$M_S(\alpha)$ and $M_L(\alpha)$ are uniquely determined by α and M_J. For example, for $S = 1/2$, $M_S(\pm) = \pm 1/2$, so $M_L(\pm) = M_J \mp 1/2$. With spinor indices, the potential matrix in Eq. (6) takes the form

$$r\mathbf{b}\cdot\mathbf{S} = rV(\theta, \phi)_{\alpha,\alpha'}. \tag{13}$$

For $S = 1/2$ atoms, the spin matrices

$$S_x = \frac{1}{2}\begin{bmatrix}0 & 1\\1 & 0\end{bmatrix}, \qquad S_y = \frac{1}{2}\begin{bmatrix}0 & -i\\i & 0\end{bmatrix}, \qquad S_z = \frac{1}{2}\begin{bmatrix}1 & 0\\0 & -1\end{bmatrix} \tag{14}$$

lead to a potential matrix of the form

$$rV = -r\mathbf{b}\cdot\mathbf{S} = -r\begin{bmatrix}\cos\theta & \dfrac{-\sin\theta\exp(-i\phi)}{2}\\ \dfrac{-\sin\theta\exp(i\phi)}{2} & -\cos\theta\end{bmatrix}. \tag{15}$$

We obtain coupled equations in r by introducing Eqs. (12) and (13) into Eq. (6), followed by multiplication on the left-hand side by $rY[L', M_L(\alpha'); \theta, \phi]\eta(\alpha')^\dagger$, then integration over θ, ϕ and contraction over the spinor indices, using Eqs. (10) and (11). Explicitly,

$$r\sum_{\beta',L,\beta,\alpha}\int d\Omega Y[L', M_L(\alpha'); \Omega]^*\eta(\alpha')_{\beta'}{}^\dagger \times [(\nabla^2 + 2E)\delta(\beta', \beta) + 2rV(\Omega)_{\beta'\beta}]r^{-1}R(r)_{L\alpha}Y[L, M_L(\alpha);\Omega] \times \eta(\alpha)_\beta = \sum_{L,\alpha}\left\{\left[\frac{d^2}{dr^2} - \frac{L(L+1)}{r^2} + 2E\right]\delta(\alpha', \alpha)\delta(L', L) - 2r\tilde{V}_{L'\alpha',L\alpha}\right\}R(r)_{L\alpha} = 0. \tag{16}$$

The matrix $V(\theta, \phi)_{\alpha'\alpha}$ becomes a matrix over L, $\tilde{V}_{L'\alpha',L\alpha}$. For $S = 1/2$, with $\alpha = \pm$, the matrix elements are

$$\tilde{V}_{L'\pm,L\pm} = \mp\langle Y[L', M_L(\pm)]|\cos\theta|Y[L, M(\pm)]\rangle \tag{17}$$

and

$$\tilde{V}_{L'\pm,L\mp} = \langle Y[L', M(\pm)]\left|\frac{\sin\theta\exp(\pm i\phi)}{2}\right|Y[L, M(\mp)]\rangle. \tag{18}$$

The Schrödinger equation that results may be written compactly as

$$\left[\frac{d^2}{dr^2} - Dr^{-2} + 2(E - r\tilde{V})\right]R = 0, \tag{19}$$

where

$$D_{L'\alpha',L\alpha} = L(L+1)\delta(L', L)\delta(\alpha', \alpha). \tag{20}$$

If the expansion (12) involves N_c values of $L\alpha$, R becomes an $N_c \times N_c$ matrix that we take to be diagonal in the limit $r \to 0$.

In the limit $r \to 0$, where $r\tilde{V}$ is negligible and the $L(L+1)r^{-2}$ term from ∇^2 dominates, the $R_{L\alpha}$ basis is convenient. On the other hand, for the limit $r \to \infty$, the asymptotic phase shift and normalization factors are more easily computed with the help of a frame transformation that diagonalizes $\tilde{V}_{L\eta,L\eta'}$. In the following expression, i, j, and k denote direct product combinations of L and α:

$$\sum_{j,k} P_{ij}^{\dagger} \tilde{V}_{jk} P_{kl} = \Lambda_{ij} \delta_{ij}. \tag{21}$$

The corresponding transformation of the diagonal D matrix term leads to a nondiagonal matrix C:

$$\sum_{j,k} P_{ij}^{\dagger} D_{jk} \delta_{jk} P_{kl} = C_{il}. \tag{22}$$

Thus, for the transformed state vectors ϕ, where

$$P^{\dagger} R = \phi, \tag{23}$$

the Schrödinger equation becomes

$$\left[\frac{d^2}{dr^2} - Cr^{-2} + 2(E - r\Lambda)\right]\phi = 0, \tag{24}$$

ϕ is also an $N_c \times N_c$ matrix.

Asymptotically, each element of ϕ is a linear combination of the Ai and Bi solutions to the Airy equation, with arguments determined by the eigenvalues Λ_{ii} of $\tilde{V}$:

$$z(i, r) = (2\Lambda_{ii})^{1/3}\left(r - \frac{E}{\Lambda_{ii}}\right). \tag{25}$$

For the closed channels, $\Lambda_{ii} > 0$; hence $z(i, r) > 0$, and ϕ_{ij} rises or falls exponentially as $\exp[\pm 2z(i, r)^{3/2}/3]$. For $\Lambda_{ii} < 0$, the Ai and Bi functions oscillate. Asymptotically, we can write

$$\phi \rightarrow Bi[z(r)]B + Ai[z(r)]A, \tag{26}$$

where Bi and Ai are diagonal matrices and the matrices A and B approach constant values as $r \rightarrow \infty$.

The numerical solution of Eqs. (19)–(24) is complicated by the stiff problem: When rapidly rising and oscillatory components are coupled together, the more rapidly rising components tend to dominate, leading to loss of numeric information about other components. In the present context, two remedies developed by Johnson[18,19] apply. In either case the useful information is contained in the log-derivative matrix, $y = \phi' \phi^{-1}$. Using relation (26), one can write

$$y = [Bi'(r) + Ai'(r)K][Bi(r) + Ai(r)K]^{-1}, \tag{27}$$

where $K = AB^{-1}$. In Eq. (27), primes denote differentiation with respect to r, and we have abbreviated the arguments of the Airy functions: $Ai(r) \equiv Ai[z(r)]$. K may be partitioned into submatrices that span the open and closed channels and connect these two manifolds:

$$K = \begin{bmatrix} K_{oo} & K_{oc} \\ K_{co} & K_{cc} \end{bmatrix}. \tag{28}$$

As shown by Johnson[18] for the normal case of potentials that tend to a constant as $r \rightarrow \infty$, the above definition of the closed-channel asymptotic basis functions gives a scattering matrix (defined only for the open channels) that involves only the submatrix K_{oo}:

$$S_{oo} = (1 + iK_{oo})^{-1}(1 - iK_{oo}). \tag{29}$$

Futhermore, it can be shown that, with the above definitions, K_{oo} is obtained from only the open–open submatrix of y and from the open-channel Airy functions:

$$K_{oo} = [Ai'(r) - y(r)_{oo} Ai(r)]^{-1}[y(r)_{oo} Bi(r) - Bi'(r)]. \tag{30}$$

The first method presented by Johnson[18] for the computation of the y matrix was by transformation to the Ricatti equation in y. The Ricatti equation corresponding to the Schrödinger equation (24) is

$$y_{\phi}' + [Cr^{-2} + 2(E - \Lambda r)] + y_{\phi}^2 = 0. \tag{31}$$

Johnson's algorithm for numerical solution of the Ricatti equation[18] has been widely used in atomic physics.[20] The second method is known as the "renormalized Numerov method,"[19] in which the Schrödinger equation is solved effectively for the ratio of the wave function at two successive mesh points. The log-derivative matrix, y, is obtained from this ratio. By successive multiplications, it is possible to recover ψ, but when this is done the rapidly rising components again dominate, so eventually the columns of ϕ become dependent, and information about other components is lost. Because it is necessary to integrate to the asymptotic limit such that the off-diagonal terms in Cr^{-2} are negligible to obtain correct normalization, we have not been able to obtain reliable wave functions by the renormalized Numerov integration method. However, K matrices obtained by the two methods agree well.

To obtain good estimates for the asymptotic value of the phase shifts, $\delta_{ij} = \tan^{-1}K(r)_{ij}$ is obtained at three sufficiently large values r_{α}, and then a power-law extrapolation of the form $\delta(r) = a + br^{-\beta}$ is used. For large L_{max} [Eq. (12)], off-diagonal terms in Cr^{-2} originating from centrifugal terms $L(L + 1)r^{-2}$ require larger values of r_{α}. Values for r_{α} varied between 30 and 200. The step size was typically 0.01 or 0.02 for six through nine channels but had to be decreased as the number of channels increased. With more channels, N_c, the matrix inversions required for each step, can be expected to increase CPU requirements approximately as N_c^2. However, since the integration must go to larger values of r with larger L_{max}, and also the increment must decrease, the computational expense increases at least as N_c^3. With $N_c = 6$, integration for each energy value required ~20 sec of IBM 3090 CPU time.

The standard theory of scattering in spherically symmetric central potentials that tend to a constant as $r \rightarrow \infty$ provides a method of identifying resonance states from the

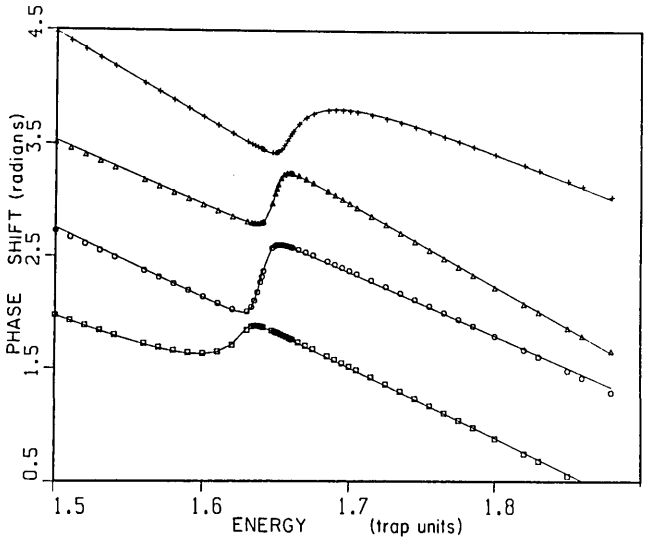

Fig. 2. Eigenphases as a function of energy for $S = 1/2$, $M_J = 5/2$, showing the effect of a resonance at 1.63 trap units. The solid curves represent a fit as discussed in the text.

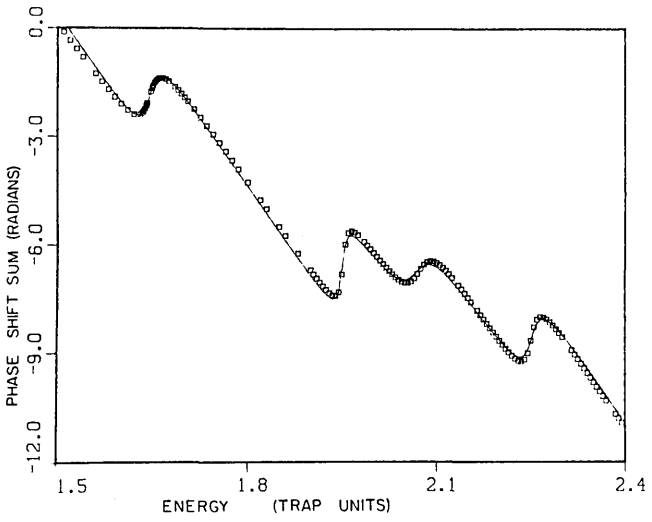

Fig. 3. Sum of eigenphases for $S = 1/2$, $M_J = 5/2$, with results of a fit to Eq. (32) (solid curve).

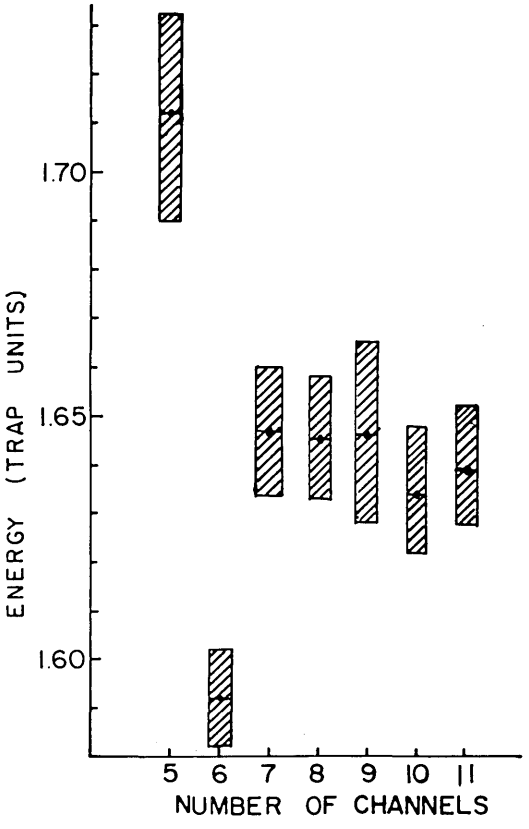

Fig. 4. Resonance energy and width (shown as the extent of the hatched regions) for the lowest $M_J = 5/2$ resonance as a function of the number of channels included in the calculation.

behavior of the asymptotic phase shift, δ. δ may be represented by a slowly varying background term plus terms that rise by π as the energy passes through a resonance:

$$\delta = \delta_{bg} + \sum_i \tan^{-1}\left[\frac{\Gamma_i}{2(E - E_j)}\right], \tag{32}$$

where E_i is the energy and Γ_i the width of resonance i. In this case, the asymptotically independent solutions (independent channels) of Eq. (24) are coupled by the r^{-2} terms, similar to the coupling of J, L channels in quantum-defect theory by core interactions and spin–orbit effects. The plot of eigenphases as a function of energy in Fig. 2 resembles plots of phase shifts in strongly coupled multichannel situations, either in quantum-defect analyses or in atomic scattering theory.[21] The solid curve represents a fit to the computed points with a function obtained by diagonalizing a model matrix of eigenphase shifts. The diagonal elements in this matrix were given a linear variation with energy plus a resonance term of the form given in Eq. (32) for one channel. The model also includes coupling terms between the resonance channel and the others. Figure 2 shows that the data fit this model quite well. This model appears to be similar to that discussed by Burke *et al.*,[22] Macek,[23] and Hazi[24] in connection with multichannel atomic scattering. The contribution of the various asymptotic channels to the resonance wave function is indicated by the fitted coupling elements or by the spacings between the $\delta(E)$ functions for each eigenphase.[23,24]

However, for purposes of extracting resonance parameters it is simpler to consider the sum of eigenphases, which has been shown by Hazi[24] to obey the expression for the single-channel phase shift, Eq. (32). Again the background term varies linearly with energy. Figure 3 shows an example of a fit to the eigenphase sum over a wider region of energy for the same $S = 1/2$, $M_J = 5/2$ manifold portrayed in Fig. 2. By adjusting the energy and width for each resonance and two parameters for δ_{bg}, an excellent fit to the sum of the eigenphases is usually obtained.

We found one puzzling case, the lowest resonance in the $M_J = 3/2$ manifold, in which the phase shifts exhibit a sharp dip rather than a jump. This appeared only when an odd number of channels was used in the calculation. For $S = 1/2$ atoms, an odd number of channels implies that L_{max} is the same for the two M_S components, while with an even number of channels the number of L terms in each spinor component is the same. For all other resonances, the phase shifts obtained with an odd number of channels exhibited the same behavior as shown in Fig. 3, and the sum of the eigenphases could be fitted to Eq. (32).

A test of the convergence of the above computational procedure with the number of channels is shown in Fig. 4 for the lowest resonance with $M_J = 5/2$. In Fig. 4 the calculated resonance energy values fall well within the width if more than six channels are used for the calculation. Higher-lying resonances of course will contain more high-L character and therefore converge more slowly.

4. CALCULATION OF DISCRETE QUANTUM LEVELS IN THE ADIABATIC APPROXIMATION

As we mentioned above, it is possible to diagonalize the potential matrix that occurs in Eq. (6) by applying a succession of rotation operators:

$$V_D = U(\theta, \phi)^\dagger \mathbf{b} \cdot \mathbf{S} U(\theta, \phi) = |\mathbf{b}| S_z, \tag{33}$$

where

$$U(\theta, \phi) = \exp(-i\phi S_z)\exp(i\theta_B S_y)\exp(i\phi S_z), \tag{34}$$

in which

$$\theta_B = \cos^{-1}\frac{B_z}{|\mathbf{B}|} = \cos^{-1}\left[\frac{\cos\theta}{(\cos^2\theta + \sin^2\theta/4)^{1/2}}\right]. \quad (35)$$

We note that $[U(\theta, \phi), J_z] = 0$. Effectively, at each point in space it rotates the spin vector so as to orient it parallel to the local direction of the magnetic field. The diagonal elements of $r|\mathbf{b}|S_z$ represent the potential seen by the atom when it remains in a given M_S state with respect to the local field direction. Hence we may say that the adiabatic potential for the M_S state is

$$V_D(M_S, M_S') = M_S r(\cos^2\theta + \sin^2\theta/4)^{1/2}\delta(M_S, M_S'). \quad (36)$$

The transformation of the kinetic energy term by $U(\theta, \phi)$ results in several additional terms proportional to r^{-2}, as shown in Appendix A. Some of these terms couple states of different M_S and hence introduce nonadiabatic effects that lead to ejection from the trap. If one ignores the discrete-continuum coupling terms in $U^\dagger\nabla^2 U$, energies and wave functions for purely discrete quantum levels may be computed rather easily. The diagonal terms in $U^\dagger\nabla^2 U$ have the effect of adding a repulsive potential proportional to r^{-2} in addition to $L(L+1)r^{-2}$, the usual centrifugal repulsive potential. These additional repulsive terms can be understood as decreasing the probability that an atom passes near the origin without a change of M_S, defined with respect to the local field direction.

Although V_D is not separable in any coordinate system, the separable part may be considered a zeroth-order Hamiltonian and the nonseparable part a perturbation. We have used both a cylindrical and a spherical coordinate representation for this calculation. In spherical coordinates, the solution procedure again involves an expansion of the form given in Eq. (10) for each of the spinor components. For discrete states we are concerned only with sublevels $M_S > 0$. Multiplication by $Y(L, M)$ again reduces the problem to coupled equations:

$$\sum_{L,M_S}\left\{\frac{d^2}{dr^2} - F(L', M_S'; L, M_S)r^{-2} + 2[E - G(L', M_S'; L, M_S)r]\right\}S(r)_{L,k}\eta(M_S) = 0, \quad (37)$$

where the radial wave function is now denoted $S(r)$ to distinguish it from the solution to Eqs. (14) and $\eta(M_S)$ denotes the spinor component. The various possible eigenfunctions are denoted k. For a manifold of given M_J,

$$F(L', M_S'; L, M_S) = \int d\Omega Y(L', M_L'; \Omega)\eta(M_S')\delta(M_L' + M_S' - M_J) \times \left(\sum_{i=0}^{8} f_i\right) Y(L, M_L; \Omega)\eta(M_S)\delta(M_L + M_S - M_J), \quad (38)$$

where f_i, $i = 1, 8$ are given in Appendix A and

$$f_0 = L(L+1)\delta(L', L)\delta(M_S', M_S) \quad (39)$$

is identical with D [Eq. (20)]. Also,

$$G(L', M_S'; L, M_S) = \int d\Omega Y(L'M_L'; \Omega)\delta(M_L' + M_S' - M_J)(\cos^2\theta + \tfrac{1}{4}\sin^2\theta)^{1/2} \times M_S Y(L, M_L; \Omega)\delta(M_L + M_S - M_J)\delta(M_S', M_S), \quad (40)$$

so that G is diagonal in M_S.

The discrete states are obtained by first taking the diagonal elements of Eq. (30) as a zeroth-order Hamiltonian potential term:

$$V_0(L', M_S'; L, M_S) = [F(L, M_S; L, M_S)r^{-2} - 2G(L, M_S; L, M_S)r] \times \delta(L', L)\delta(M_S', M_S). \quad (41)$$

From this potential, one computes a series of eigenfunctions for each $M_S > 0$ and each $L \geq M_L$, where $M_L = M_J - M_S$, up to some cutoff energy and some cutoff L_{max}. All the nondiagonal terms in F and G are then evaluated between these basis functions and introduced into a Hamiltonian matrix, which is diagonalized to obtain the eigenenergies. In computing the lowest eigenvalues of several S, M_J manifolds presented below, we have used typically 5 L values in the sum and 50 basis functions. The basis functions were computed with the Numerov integration method, with typically 2000 grid points. Although the limit as cutoff energy and L become large is difficult to establish analytically, convergence appears to be satisfactory.

5. RESULTS AND CONCLUSION

Resonance energies and widths for $S = 1/2$ atoms in a quadrupole trap are shown in Fig. 5 for various values of M_J, the component of total angular momentum around the symmetry axis. The hatched regions denote the boundaries $E_i \pm \Gamma_i/2$. For each M_J manifold except $M_J = 1/2$, the results for discrete energies from the purely adiabatic approach are indicated to the left of the resonances. It is curious that the effect of the continua is to raise the energies by roughly a constant amount. For $M_J = 1/2$, singularities in the matrix elements (see above and Appendix A) preclude a calculation with the adiabatic approach.

One important conclusion from Fig. 5 is that, even for some $M_J = 1/2$ resonances, the widths are less than the spacing. For higher M_J, the widths are relatively narrower because the atoms avoid the $\mathbf{B} = 0$ point at the origin where nonadiabatic transitions occur. The widths for a given M_J manifold exhibit only statistical fluctuations about a mean value that depends on M_J approximately as $0.5 \times 3^{(-M_J)}$ (to within a factor of 2). Hence the quantum levels should be resolvable, with narrow resonances of higher M_J standing on broader resonances of lower M_J. The level structure could probably be observed, for example, by optical detection of microwave transitions from one hyperfine level to another, similar to means used recently to detect resonance transitions between Zeeman sublevels of a single hyperfine level.[8]

The spectral transition intensities, which are not calculated in the present study, will depend on the average orientation of the spin with respect to the microwave magnetic field. Clearly, the density of resonance transitions will be formidable unless the trapped atoms are cooled to a temperature corresponding to no more than the trap energy unit, dis-

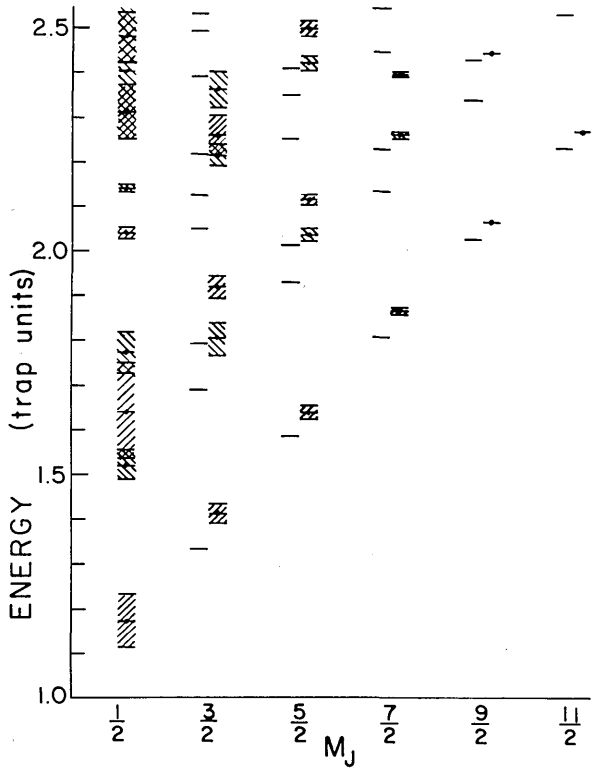

Fig. 5. Resonance energies and widths for $S = 1/2$ atoms in a magnetostatic trap in terms of trap units defined below Eqs. (4). The hatched regions denote the resonance widths. For all but the $M_J = 1/2$ manifold, the discrete energies calculated by neglecting continuum levels are given to the left of the resonance energies.

cussed in connection with Table 1. It is a matter of conjecture whether evaporative cooling, which has been used for trapped spin-aligned hydrogen atoms,[25] can be used to cool atoms in the quadrupole trap below the recoil limit.

With regard to the possibility of observing narrow spectroscopic transitions between quantum levels in the trap, we note that if the trap energy unit is 2 kHz, the widths of the $M_J = 9/2$ levels, for example, are ~10 Hz (0.005 trap unit). This might be compared with 50-Hz line widths that have been obtained with cold cesium atoms in free fall[26] or with 2-Hz linewidths obtained in fountain experiments with cold sodium atoms.[27] Linewidths for higher M_J levels in the trap will be narrower, but if there is thermal equilibration between different M_J values the fractional populations will be less. However, if the kinetic energy of atoms in the trap can be reduced without relaxing M_J, then the stabler levels will have relatively more population.

The resonance widths also establish a time scale for the study of Bose–Einstein condensation in a quadrupole trap. Again for a trap energy unit of 2 kHz, the width of the lowest $M_J = 1/2$ resonance of 0.13 trap unit corresponds to a decay time of 0.6 msec, which must be long compared with the cooling process. Although this time is indeed long compared with optical cooling time scales, it is probably slow compared with the time required for evaporative cooling. If one can produce Bose–Einstein condensation into the lowest level of a manifold of higher M_J, the time scale can be considerably lengthened.

In view of the correlation for $S = 1/2$ and $M_S > S$ between the discrete eigenvalues and the resonance energies including continuum interactions, we present in Fig. 6 the discrete energies for $S = 1$ and $S = 2$ to indicate the spacing of the trap quantum levels for alkali atoms. We do not have results with the many-channnel coupled equations for these cases, so widths cannot be given. For $S = 2$, the lowest energy levels are predominantly $M_S = 1$. At energies approximately three units above the lowest level of each manifold, the energy-level density increases relative to the $S = 1$ distribution owing to the onset of the $M_S = 2$ resonances. That the first excitation energy is always approximately 0.5 unit reflects the definition of trap unit of energy [Eqs. (7)].

Similar computational methods could be used for $|\mathbf{B}|_{\min} \neq 0$ traps, which have a quadratic rather than a linear potential variation near the center, in order to determine the loss rate as a function of $|\mathbf{B}|_{\min}$.

APPENDIX A

When the transformation $U(\theta, \phi)$ [Eq. (34)] is applied to the Laplacian operator, additional terms proportional to r^{-2} result:

$$U(\theta, \phi)^{\dagger} \nabla^2 U(\theta, \phi) = \nabla^2 - r^{-2} \sum_{i=1}^{8} f_i. \tag{A1}$$

Unlike usual rotation operators that commute with the Laplacian, this transformation produces additional terms because the parameters of the rotation are functions of θ and ϕ. Effectively, the rotational transformation U is applied to orthogonal axes constructed on the surface of the unit sphere, and it depends on the particular location on the sphere. The eight terms in the sum are

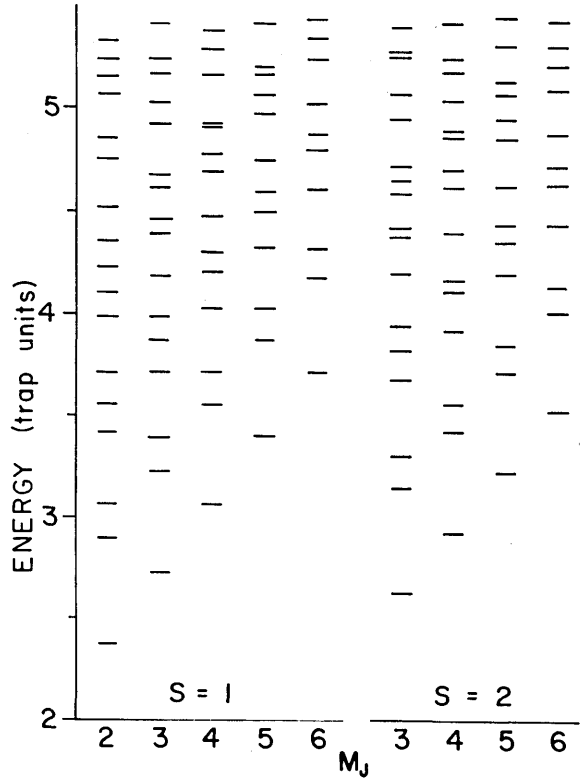

Fig. 6. Discrete energies, neglecting couplings with continuum levels, for $S = 1$ and $S = 2$.

$$f_1 = S_z^2 + 2S_zJ_z,$$

$$f_2 = \left[\frac{1}{4(1+3\cos^2\theta)} + \frac{1}{(1+3\cos^2\theta)^2}\right](S_+S_- + S_-S_+),$$

$$f_3 = \left(\frac{4\cot^2\theta}{1+3\cos^2\theta}\right)S_z^2,$$

$$f_4 = \left[\frac{4\cos\theta}{\sin^2\theta(1+3\cos^2\theta)^{1/2}}\right]S_zJ_z,$$

$$f_5 = \left[\frac{\cos\theta(4+3\sin^2\theta)}{\sin\theta(1+3\cos^2\theta)^2} + \frac{2}{1+3\cos^2\theta}\right]\frac{\partial}{\partial\theta} \times [S_-\exp(i\phi) - S_+\exp(-i\phi)],$$

$$f_6 = \left[\frac{\cos\theta}{\sin\theta(1+3\cos^2\theta)}\right]\{S_-\exp(i\phi) + S_+\exp(-i\phi)]S_z + S_z[S_-\exp(i\phi) + S_+\exp(-i\phi)]\},$$

$$f_7 = \left[\frac{1}{\sin\theta(1+3\cos^2\theta)^{1/2}}\right][S_-\exp(i\phi) + S_+\exp(-i\phi)]J_z,$$

$$f_8 = \left[\frac{1}{4(1+3\cos^2\theta)} - \frac{1}{(1+3\cos^2\theta)^2}\right] \times [S_+^2\exp(-2i\phi) + S_-^2\exp(2i\phi)]. \quad \text{(A2)}$$

The first four terms connect states of the same M_S, terms 5, 6, and 7 connect states $\Delta M_S = \pm 1$, and the last term connects states with $\Delta M_S = \pm 2$. The denominators $\to 0$ for $\theta = 0$ and π. This creates no problems for matrix elements between states with $L > 0$, since the two $\sin\theta$ factors in the $Y(LM)$ then cancel the $\sin\theta$ or $\sin^2\theta$ in the denominator. However, for matrix elements with $L = 0$, the integrals over θ and ϕ will diverge, invalidating the use of this transformation for the $M_J = S$ manifold.

ACKNOWLEDGMENTS

We are indebted to Thomas Hagstrom, Joseph Macek, and John Delos for crucial bits of advice and to Howard Sporn for useful conversations. Some of the calculations were performed at the Cornell National Supercomputer Facility, which receives funding from the National Science Foundation, IBM, New York State, and members of the Cornell Theory Center's Corporate Research Institute. Principal support is from the U.S. Office of Naval Research and the National Science Foundation.

* Present address, Photometrics, Inc., 4 Arrow Drive, Woburn, Massachusetts 01801.

† Undergraduate summer research assistant; present address, McGill University, Montreal, Canada.

REFERENCES

1. P. D. Lett, R. N. Watts, C. I. Westbrook, W. D. Phillips, P. L. Gould, and H. J. Metcalf, "Observation of atoms laser cooled below the Doppler limit," Phys. Rev. Lett. **61**, 169–172 (1988).
2. J. Dalibard, C. Salomon, A. Aspect, E. Arimondo, R. Kaiser, N. Vansteenkiste, and C. Cohen-Tannoudji, "New schemes in laser cooling," in *Proceedings of the Eleventh International Conference on Atomic Physics* (World Scientific, Singapore, 1988); A. Aspect, E. Arimondo, R. Kaiser, N. Vansteenkiste, and C. Cohen-Tannoudji, "Laser cooling below the one-photon recoil energy by velocity-selective coherent population trapping," Phys. Rev. Lett. **61**, 826–829 (1988).
3. Y. Shevy, D. S. Weiss, P. J. Ungar, and S. Chu, "Bimodal speed distribution in laser-cooled atoms," Phys. Rev. Lett. **62**, 1118–1121 (1989).
4. V. Bagnato, D. E. Pritchard, and D. Kleppner, "Bose–Einstein condensation in an external potential," Phys. Rev. A **35**, 4354–4358 (1987).
5. D. E. Pritchard, "Cooling neutral atoms in a magnetic trap for precision spectroscopy," Phys. Rev. Lett. **51**, 1336–1339 (1983).
6. T. Bergeman, G. Erez, and H. J. Metcalf, "Magnetostatic trapping fields for neutral atoms," Phys. Rev. **35**, 1535–1546 (1987).
7. A. L. Migdall, J. V. Prodan, W. D. Phillips, T. H. Bergeman, and H. J. Metcalf, "First observation of magnetically trapped neutral atoms," Phys. Rev. Lett. **54**, 2596–2599 (1985).
8. A. G. Martin, K. Helmerson, V. S. Bagnato, G. P. Lafyatis, and D. E. Pritchard, "Rf spectroscopy of trapped neutral atoms," Phys. Rev. Lett. **61**, 2431–2434 (1988).
9. See for example, M. S. Child, "Predissociation and photodissociation of IBr: a case of intermediate coupling strength," Mol. Phys. **32**, 1495–1510 (1976).
10. R. R. Lewis, Department of Physics, University of Michigan, Ann Arbor, Michigan 48109 (personal communication).
11. J. Schwinger, "On nonadiabatic processes in inhomogeneous fields," Phys. Rev. **51**, 648–651 (1937).
12. J. Schwinger, "Is spin coherence like Humpty Dumpty?" in *Proceedings of the Eleventh International Conference on Atomic Physics* (World Scientific, Singapore, 1988).
13. M. O. Scully, R. Shea, and J. D. McCullen, "State reduction in quantum mechanics: a calculational example," Phys. Rep. **43**, 485–498 (1978).
14. See, for example, A. O. Barut, M. Bozic, Z. Marie, and H. Rausch, "Tunneling of neutral spin-1/2 particles through magnetic fields," Z. Phys. A **328**, 1–10 (1987).
15. U. Bonse and H. Rauch, eds., *Neutron Interferometry* (Clarendon, Oxford, 1979).
16. H. J. Metcalf, "Magneto-optical trapping and its application to helium metastables," J. Opt. Soc. Am. B **6**, 2206 (1989).
17. M. V. Berry, "Quantal phase factors accompanying adiabatic changes," Proc. R. Soc. London Ser. A **392**, 45–57 (1984).
18. B. R. Johnson, "The multichannel log-derivative method for scattering calculations," J. Comp. Phys. **13**, 445–449 (1973); "Comment on a recent criticism of the formula used to calculate the S matrix in the multichannel log-derivative method," Phys. Rev. A **32**, 1241–1242 (1985).
19. B. R. Johnson, "New numerical methods applied to solving the one-dimensional eigenvalue problem," J. Chem. Phys. **67**, 4086–4093 (1977); "The renormalized Numerov method applied to calculating bound states of the coupled-channel Schrödinger equation," J. Chem. Phys. **69**, 4678–4688 (1978).
20. See, for example, T. G. Heil and J. B. Sharma, "Differential cross sections for the charge-transfer Reaction $O^{2+} + He \to O^+ + He^+$ at low energies," Phys. Rev. A **36**, 3669–3673 (1987).
21. U. Fano and A. R. P. Rau, *Atomic Collisions and Spectra* (Academic, New York, 1986), especially Chap. 8.
22. P. G. Burke, J. Cooper, and S. Ormonde, "Low energy scattering of electrons by helium," Phys. Rev. **183**, 245–264 (1969).
23. J. Macek, "Behavior of eigenphases near a resonance," Phys. Rev. A **2**, 1101–1103 (1970).
24. A. Hazi, "Behavior of the eigenphase sum near a resonance," Phys. Rev. A **19**, 920–922 (1979).
25. N. Masuhara, J. Doyle, J. Sandberg, D. Kleppner, T. Greytak, H. Hess, and G. Kochanski, Phys. Rev. Lett. **61**, 935–938 (1988).
26. D. W. Seisko and C. E. Wieman, Opt. Lett. **14**, 269–271 (1989).
27. S. Chu, Department of Physics, Stanford University, Stanford, California 94305 (personal communication of work submitted for publication, 1989).